Final Technical Report

SATELLITE SAR REMOTE SENSING OF THE GREAT LAKES ICE COVER

Assigned Project No. 56

TO

NATIONAL OCEANIC AND ATMOSPHERIC ADMINISTRATION

NOAA Code E/SP

4700 Silver Hill Road

Stop 9909

Washington, D.C. 20233-9909

S. V. Nghiem[†], G. A. Leshkevich[‡], and R. Kwok[†]

[†]Jet Propulsion Laboratory

California Institute of Technology

Pasadena, California 91101

[‡]Great Lakes Environmental Research Laboratory

National Oceanic and Atmospheric Administration

Ann Arbor, Michigan 48105

August 1998

Table of Contents

Satellite SAR Remote Sensing of the Great Lakes Ice Cover

S. V. Nghiem[†], G. A. Leshkevich[‡], and R. Kwok[†]

[†]Jet Propulsion Laboratory, MS 300-235
California Institute of Technology
4800 Oak Grove Drive
Pasadena, California 91109
Tel: 818-354-2982, Fax: 818-393-3077
E-mail: nghiem@solar.jpl.nasa.gov
ron@rgps1.jpl.nasa.gov

[‡]NOAA/Great Lakes
Environmental Research Laboratory
2205 Commonwealth Boulevard
Ann Arbor, Michigan 48105
Tel: 313-741-2265, Fax: 313-741-2055
E-mail: leshkevich@sparc.glerl.noaa.gov

I. OBJECTIVE

The main objective of this project is to map the Great Lakes ice cover using radar data acquired by satellite Synthetic Aperture Radar (SAR) data such as RADARSAT or ERS SAR. ERS is a European satellite and RADARSAT is a Canadian satellite on sun-synchronous near-polar orbits. ERS carries a SAR with the vertical polarization and RADARSAT has a SAR with the horizontal polarization. Both SARs operate at C-band frequency, which image ice cover on the Great Lakes during winter seasons. ERS SAR Precision Image (PRI) data over the Great Lakes were received at the Gatineau station and processed by the German Processing and Archiving Facility (D-PAF). RADARSAT data were acquired in ScanSAR Wide A (SWA) mode and were also received at the Gatineau station. In the SWA mode, the data calibration is more involved because several antenna beams are mosaiced together to form an image covering an area of 500 km by 500 km on the ground.

II. PROGRESS

A. Algorithm Development

We have developed the first algorithm for lake ice mapping using RADARSAT pre-release scenes of the ice cover in the 1996 winter. The SAR images were displayed and analyzed on a Unix computer. We used field photographs along with ice charts and field notes to interpret and analyze ice types and patterns seen in the SAR images. The pre-release scenes received from the Gatineau readout station had the scalloping or banding effects due to uncalibrated effects of antenna patterns of the different beams. This is evident in both the ScanSAR Wide and ScanSAR Narrow images in Figures 1 and 2, respectively.

Although training sets were taken and processed within an image band, they could not be used to classify the entire scene because results of the classification outside the band in which the training set was taken could be subject to error. At the present time, ScanSAR images have not been calibrated to fully eliminate the scalloping effects. Currently, data over taiga forest are being ordered by the Alsaka SAR Facility (ASF) for RADARSAT SWA calibration; however, ASF plan for SWA calibration processing is delayed to 1999. Once the SWA calibration processor is completed, SWA data acquired over the Great Lakes can be calibrated to remove the banding effects.

To test the ice mapping algorithm, a supervised level slicing classification [*Lillesand and Kiefer*, 1979] was used based on a comparison of brightness or digital values in the SAR scene representing known ice types as identified on the ground [*Leshkevich et al*, 1994, 1995]. With field observations and ancillary data, two ice types (snow ice and new ice) and open water were identified in the computer displayed SAR image and a representative training set, consisting of a range of digital values, for each type was extracted. A color was assigned to each type (range of values). Then, the color assigned to each range was applied to the entired scene producing a color-coded classified image. This method requires a manual selection of training areas and it is applicable to an uncalibrated SAR image.

However, as explained above, the classification is only valid for the image band in which the training set was taken. Ice mapping results using uncalibrated RADARSAT SAR image will be shown in section II.E. For calibrated ERS SAR image, the ice classification and mapping based on calibrated backscatter values in the SAR scene are done automatically using a backscatter signature library for different ice types and the results will be presented in section II.F. Radar signatures of ice are obtained from field experiments described in the next section.

B. Field Experiments

To continue the development and validation of the algorithm for remote sensing of Great Lakes ice using satellite SAR data, we conducted two experiments during the 1997 winter season across the Straits of Mackinac and Lake Superior. The experimental campaign was coordinated into two expeditions on two different United States Coast Guard (USCG) Ice Breaker vessels, the Biscayne Bay in February and the Mackinaw (an Arctic-class ice breaker) in March. The particular objective of these experiments are to measure radar backscatter signatures of various ice types and open water together with ground truth data to establish a backscatter library that can be used to translate SAR data into ice maps. Such a comprehensive radar data set does not exist in the open literature and these experiments provide the first radar signature data set for Great Lake ice remote sensing.

In these experiments, the Jet Propulsion Laboratory (JPL) polarimetric scatterometer was mounted on board the Biscayne Bay and the Mackinaw to measure the backscatter. The JPL scatterometer [*Nghiem*, 1993, *Nghiem et al.*, 1997] is an accurate radar capable of detecting a small pin in the far field. The operating frequency is in C band, which is the same frequency band of many remote sensing satellite SARs including RADARSAT SAR. Furthermore, the JPL scatterometer has the full polarization capability including both magnitude and phase measurements. Thus, the results are applicable not only to RADARSAT SAR with the horizontal polarization, but also with ERS SAR with the vertical polarization and the future ENVISAT SAR with multiple polarizations.

The JPL radar system was delivered at the National Oceanic and Atmospheric Administration (NOAA) Great Lakes Environmental Research Laboratory (GLERL) in early February 1997. Pre-experiment system tests and calibrations were carried out at GLERL. Then, the system was transported to the ship dock and integrated on the Biscayne Bay (2/97) and the Mackinaw (3/97). Further system tests and calibrations were performed on board the ship after the system integrations. On the Biscayne Bay, the JPL radar was mounted on the left side of the ship and the radar was controlled from the engineering control room inside the ship. A video camera was mounted on the frame of the antenna pointed in the same direction as the antenna look direction so that the ice could be observed from inside the control room on a TV monitor. The video images were recorded on 8 mm tapes and VHS VCR tapes at the same time. On the Mackinaw the radar system was also mounted on the ship left side and the radar control system was in a small room close to the radar. Figure 3 shows the radar system setup on the Mackinaw.

A Global Positioning System (GPS) receiver GARMIN GPS II unit was used to record the locations along the ship routes when the scatterometer data were taken. The GPS data were received by the unit and downloaded to the computer that controlled the radar. The data were plotted out on a map of the Great Lakes to show the locations of the ice types where radar data were obtained. The computer internal clock was synchronized with the GPS time and both radar data and GPS data were time tagged so that they can be correlated. An anemometer was used near the radar to measure in-situ wind. The ship instruments also provided location, wind data, and temperature data. Figure 4 presents the GPS data map on Lake Superior along the Mackinaw ship track.

During the experiments, accurate calibration measurements were conducted to calibrate the scatterometer data. A trihedral corner reflector of known radar cross section was used for this purpose. The corner reflector was aligned with the radar pointing direction with a laser pointer. Real time radar signals were displayed on a microwave network analyzer to check the alignment by detecting the maximum radar returns. Furthermore, another calibration target, a metallic sphere, was used to obtain additional data to validate the radar calibration. During the experiment on board the Biscayne Bay, the calibration measurements were taken while the ship docked near De Tour Village in Michigan. The calibration targets were setup on the ground and the radar was on the ship. Background measurements were used in the coherent subtraction method to remove the background noise. In the Mackinaw experiment, the calibration targets were setup on an open area at the back of the ship and microwave absorbers were used to avoid unwanted signals from reflections and multipath effects.

Ice truth data for different ice types were obtained. Ice thickness and snow thickness data were taken. Photographs showing the layering structure of snow ice and lake ice with different amount of air inclusions were taken. The photograph in Figure 5 shows an example of the ice layering structure. Wind speed and temperature were recorded. We also took a number of snow thickness measurements over an area at a location during the Biscayne Bay experiment to determine the range of snow thickness distribution. A number of photographs were taken to estimate the surface roughness condition and snow coverage. For each set of radar measurements of an ice type, photographs were taken both in the near range coincident to the area of the radar footprint and in the far range for an overall picture of the ice type.

The total duration of this year field campaign was about one month (2 weeks in 2/97 and 2 weeks in 3/97). The participants from JPL were S. V. Nghiem and R. Kwok and from NOAA/GLERL was G. A. Leshkevich. The US Coast Guard involved in this campaign were the USCG Mackinaw ice breaker, the USCG Biscayne Bay ice breaker, the USCG Traverse City Air Station, and the USCG Portage Ground Station in Michigan. The Houghton Memorial Airport provided an ideal location for the radar reflector setup and the machinery to prepare the reflector site. As described above, the Great Lakes winter experiments involved with all components including lake, ground, and space levels.

C. Shipborne Radar Data Processing

From the winter 1997 experiments, we obtained close to 2000 radar data files for various ice types for application to RADARSAT Great Lakes ice mapping. The data were acquired with the JPL C-band scatterometer on board the USCG Mackinaw and the USCG Biscayne Bay Ice Breaker Vessels as described above. For each ice type, we obtained radar data from $0°$ to $60°$ incidence angles. For each incidence angles, the measurements covered several different samples in azimuth directions scanned over the targeted area. For each antenna look direction, data were coherently averaged by 20 times over 401 samples in the frequency domain with 1 GHz bandwidth. The data included both magnitudes and phases of the scattering matrix for all combinations in the linear polarization basis.

We have applied the polarimetric scatterometer data processor, which was modified for the particular data acquisition configuration and data format for the lake ice experiments. The shipborne radar data set are calibrated both polarimetrically and radiometrically to obtain polarimetric backscattering coefficients and polarimetric covariance matrices to construct a library of backscatter signatures with multipolarizations and multi-incidence angles for the various ice types. Also, the software for antenna pattern deconvolution is modified to account for the antenna pattern effects at different incidence angles.

The fully polarimetric radar processor was completed using the system configurations and parameters for these experiments to calibrate the experimental data set to determine polarimetric covariance matrices for the various ice types. A covariance matrix includes radar backscattering coefficient σ_{HH} for horizontal polarization, copolarization ratio $\gamma = \sigma_{VV}/\sigma_{HH}$ where σ_{VV} is the vertical backscatter, crosspolarization ratio $e = \sigma_{HV}/\sigma_{HH}$ where σ_{HV} is the crosspolarized backscatter, and polarimetric coefficient ρ (both magnitude and phase) between the horizontal and vertical radar returns.

The unique feature of these backscatter data sets is that the measurements cover a large range of incidence angles ($0°$-$60°$) with all polarizations in conjunction with ice truth measurements and surface observations. The utility of these shipborne backscatter data is particularly important to current satellite SAR data such as ERS with incidence angles from $19°$ to $26°$ for vertical polarization, and RADARSAT SWA data with incidence angles from $20°$ to $49°$ for horizontal polarization. Furthermore, the multipolarization results in the data sets from these experiments will be applicable to future C-band satellite SARs such as ENVISAT and RADARSAT-2 regardless of their polarizations. An important implication from the multiple polarization radar results shown above will be discussed later for the project outlook.

D. Radar Signatures of Great Lakes Ice

We present backscatter signatures of various ice types in the Great Lakes and their use for ice mapping with satellite SAR data. For the typical ice type consisting of a snow layer on white ice over lake ice, γ is smaller than 1. Backscatter σ_{HH} is larger than σ_{VV} by 2 to 3 dB (3 dB = 200% larger) over the range of incidence angles from 30 to 60° incidence angles. An important implication of this result is that the typical ice type over the Great Lakes can be identified/mapped with the dual polarization radar data (ENVISAT SAR) because the radar signature of open water has an opposite behavior ($\gamma > 1$) regardless of wind speeds.

Deformed ice in a rubble field consists of ice plates that were pushed together by winds and waves, broken in to ice slabs of various sizes, and rafted or piled up. This ice type represents areas in the Great Lakes that are most difficult to ice breaking operations and most hazardous to commercial ship. The radar signature results show that this ice type has very strong backscatter (even brighter than typical backscatter from cities or tropical forests with large trees).

What is interesting and important from the measured signature of the rubble ice type is that the backscatter remains very strong (-5 to -3 dB) for both HH and VV polarizations over the range of incidence angles (20 to 50°) of all present and future spaceborne SARs (ERS-1, ERS-2, RADARSAT, ENVISAT, and RADARSAT-II). This result indicates that this important ice type can be identified from SAR data regardless of polarization and incidence angles. Furthermore, the backscatter is much higher that the typical backscatter equivalence noise floor of satellite SAR.

Backscatter signature results of thin black ice with bare surface or thin snow cover show that this ice type is observable at small incidence angles (less than 40°) for VV polarization (ERS SARs) due to the low radar backscatter and the noise-floor limitation of spaceborne SARs. For HH polarization such as RADARSAT SAR, observable incidence angle is around 20°. Thus, the thin black ice type is likely to be confused with calm open water. However, in terms of USCG ice breaking operations, open water or thin ice does not make much difference. We also obtained polarimetric backscatter signature of pancake ice, thick white ice, and other ice types under different snow cover and surface roughness conditions. This comprehensive radar backscatter signature data set is valuable to interpret SAR data for ice mapping over the Great Lakes.

Figures 6-8 show polarimetric backscatter data measured by the JPL C-band shipborne scatterometer during the 1997 field experiments. Figure 6 is for rough consolidated ice floes, 7 for brash ice or rubble ice field, and 8 for patchy snow cover on snow ice covered black ice [*Ice Glossary*, 1971]. These 3 ice types are often encountered in the Great Lakes. These backscatter results will be used as a backscatter signature library to map the Great Lakes ice cover with satellite SAR data. Results of ice mapping from calibrated ERS data will be shown later.

E. Ice Mapping with RADARSAT SAR Data

Since RADARSAT SWA data are not calibrated, we use visual observations of ice types from field experiments and determine their locations in the concurrent satellite image. The field observed areas are used as references (training sets) to classify ice types. This approach requires a supervised selection of training data sets from the SAR imagery. This method is applicable only to the scene acquired concurrently with the field observations within a given band of the SAR image.

A SAR image taken on 16 March 1996 over western Lake Superior is presented in Figure 2. The approximate routes of the United States Coast Guard Cutter (USCGC) *Mackinaw* and the USCGC *Neah Bay*, a smaller ice breaker that accompanied the USCGC *Mackinaw* from Sault St. Marie, Michigan to Duluth, Minnesota, are plotted on the image. In the later part of the afternoon, when the Mackinaw entered the area of the image, temperatures averaged about 2°C and winds were out of the northeast at about 7.2 m/s. Field observations from the ship were used in the ice mapping.

Training sets for two ice types and open water were applied to the scene. The ice map in Figure 9 illustrates the results of the supervised level slicing classification. The training set for open water was picked in the middle band and color-coded blue. The training set for new lake ice color-coded green and snow ice coded red were taken from the right band. Another training set for open water was also selected from the left band and color-coded yellow as the training set for open water from the middle band did not classify the open water in the left band. This is probably largely due to the radiometric differences among the bands as the areas are relatively close to each other thus likely influenced by the same wind pattern.

The analysis indicates that open water and different ice types in the ice cover can be identified, classified, and mapped in RADARSAT SAR imagery. In addition, wind has a strong influence on the backscatter from open water as observed in other RADARSAT images taken over the Great Lakes. However, uncalibrated data cannot be used to address the temporal variations and classification from scene to scene at different times and geolocations throughout the winter. In this view, calibrated SAR data are necessary.

F. Ice Mapping with ERS SAR Data

With calibrated SAR image, the backscatter signature library can be utilized for automatic ice mapping. ERS-2 SAR imagery was obtained and used for this study. A scene of the central portion of Lake Superior collected on 22 March 1997 (Figure 10) was calibrated and linear σ_0 values converted to dB according to the simplified equation for the derivation of σ_0 in Precision Image (PRI) products [*Laur et al.*, 1997). A large part of the lower right portion of the image covers land in the Keweenaw peninsula. Certain assumptions on the local incidence angle were made:

- A flat terrain is considered , i.e. there is no slope. The incidence angle depends only on the earth ellipsoid and varies from about 19.5° at near range to about 26.5° at far range (23° was used).

- Any change in incidence angle across a distributed target is neglected, i.e. a distributed target corresponds to one average value of the incidence angle.

Measured backscatter values (converted to dB) for 3 representative ice types presented in section II.D and also calm water backscatter were used as a limited backscatter library to classify and map the ice cover from the ERS imagery. The measured backscatter values for these different ice types and open water were applied to the 8 x 8 pixel averaged digital ERS-2 SAR image. The averaging not only reduced the speckle but resulted in an image similar in resolution to RADARSAT ScanSAR Wide images. The overall uncertainty is about ±1 dB due to the averaging and the incidence angle effect.

Figure 11 shows the color-coded result of the classification. Most of the ice cover in the scene was classified as rough consolidated ice floes (yellow) or brash ice (red). Areas classified as patchy snow cover on snow ice covered black ice (green) are scattered throughout the ice cover, but no calm open water was classified in the scene. This sample was measured on 23 March when we were out of the area covered by this scene. Black and gray represent unclassified a areas. The land area (Keweenaw Peninsula which can be masked out) was classified largely as brash ice (red) owing to similar backscatter intensity from the forested area. Although our route across Lake Superior appears to have passed through the northwest portion of the scene, the classification appears to be valid based on the ice types we encountered.

Another ERS scene (Figure 12) north of the above ERS scene is studied. The new scene contains Isle Royale (the large elongated feature in the image). The ice classification and mapping result is shown in Figure 13 using the same backscatter library of the 3 ice types. Further validation needs to be done on these scenes, once geo-referenced. However, this study demonstrates the capability of classifying Great Lakes ice types in calibrated satellite SAR imagery using backscatter values measured from different ice types as a ”backscatter signature library”.

III. APPLICATIONS

Results accomplished from the research in this project have been presented at several workshop and conference meetings. We have written 18 publications including 10 conference abstracts/papers, 1 occasional series paper, 4 workshop papers, and 3 technical reports. We have participated in 6 conferences and 4 workshops and organized and chaired a special session on Remote Sensing of the Great Lakes. The publications and meetings are listed in the following subsections in reverse chronological order.

A. Publications

[1] S. V. Nghiem, G. A. Leshkevich, and R. Kwok, "Shipborne Scatterometer Measurements of Great Lakes Ice," Remote Sensing for Marine and Coastal Environments, San Diego, California, October 5-7, 1998.

[2] G. A. Leshkevich, S. V. Nghiem, and R. Kwok, "Great Lakes Ice Cover Classification and Mapping Using Satellite Synthetic Aperture Radar (SAR) Data," Remote Sensing for Marine and Coastal Environments, San Diego, California, October 5-7, 1998.

[3] H. Shen, S. V. Nghiem, G. A. Leshkevich, and M. Manore, "A Summary of Current Remote Sensing and Modeling Capabilities of the Great Lakes Ice Conditions," Occasional Paper Series, Great Lakes Research Consortium, 10 p., April 1998.

[4] S. V. Nghiem, G. A. Leshkevich, and R. Kwok, "C-Band Polarimetric Backscatter Observations of Great Lakes Ice," International Geoscience and Remote Sensing Symposium, Seattle, Washington, July 6-10, 1998.

[5] G. A. Leshkevich, S. V. Nghiem, and R. Kwok, "Algorithm Development for Satellite Synthetic Aperture Radar (SAR) Classification and Mapping of Great Lakes Ice Cover," International Geoscience and Remote Sensing Symposium, Seattle, Washington, July 6-10, 1998.

[6] G. A. Leshkevich and S. V. Nghiem, "Analysis of Great Lakes Ice Cover Using RADAR-

SAT SAR Data," International Association for Great Lakes Research Conference, Hamilton, Ontario, Canada, May 18-22, 1998.

[7] S. V. Nghiem, G. A. Leshkevich, and R. Kwok, "Satellite SAR Remote Sensing of the Great Lakes Ice Cover," *Semi-Annual Rep.*, Center for Space Microelectronics Technology, Jet Propulsion Laboratory, California Institute of Technology, May, 1998.

[8] S. V. Nghiem, R. Kwok, and G. A. Leshkevich, "Satellite SAR Remote Sensing of Great Lakes Ice Cover – Backscatter Signatures and Ice Motion," Remote Sensing and Modeling Great Lakes Ice, Alexandria, Virginia, October 8-9, 1997.

[9] G. A. Leshkevich, S. V. Nghiem, and R. Kwok, "Satellite SAR Remote Sensing of Great Lakes Ice Cover – Ice Classification," Remote Sensing and Modeling Great Lakes Ice, Alexandria, Virginia, October 8-9, 1997.

[10] W. Y. Tseng, W. G. Pichel, A. K. Liu, P. Clemente-Colón, G. A. Leshkevich, S. V. Nghiem, R. Kwok, and R. R. Stone, "Near Real-Time RADARSAT Data System for NOAA CoastWatch Applications," *International Geoscience and Remote Sensing Symposium*, Singapore, August 3-8, 1997.

[11] S. V. Nghiem, G. A. Leshkevich, and R. Kwok, "Satellite SAR Remote Sensing of the Great Lakes Ice Cover," *Annual Rep.*, Center for Space Microelectronics Technology, Jet Propulsion Laboratory, California Institute of Technology, August, 1997.

[12] S. V. Nghiem and G. A. Leshkevich, "The Impact of Great Lakes Ice and the Lake Ice Remote Sensing from Space," *Progress In Electromagnetics Research Symposium*, Cambridge, Massachusetts, July 7-11, 1997.

[13] G. A. Leshkevich, S. V. Nghiem, and R. Kwok, "Algorithm Development for Satellite SAR Mapping of Great Lakes Ice Cover," *Progress In Electromagnetics Research Symposium*, Cambridge, Massachusetts, July 7-11, 1997.

[14] G. A. Leshkevich, S. V. Nghiem, and R. Kwok, "Satellite SAR Remote Sensing of

Great Lakes Ice Cover Using RADARSAT Data," *Workshop on Remote Sensing of Planetary Ices: Earth and Other Solid Bodies*, Flagstaff, Arizona, June 11-13, 1997.

[15] S. V. Nghiem, R. Kwok, and G. A. Leshkevich, "Satellite SAR Remote Sensing of the Great Lakes Ice Cover," *Semi-Annual Rep.*, Center for Space Microelectronics Technology, Jet Propulsion Laboratory, California Institute of Technology, April, 1997.

[16] G. A. Leshkevich, S. V. Nghiem, and R. Kwok, "Satellite SAR Remote Sensing of Great Lakes Ice Cover Using RADARSAT Data," *Proceedings of the Fourth International Conference on Remote Sensing for Marine and Coastal Environments*, Vol. I, pp. 126-134, Orlando, Florida, March 17-19, 1997.

[17] G. A. Leshkevich, S. V. Nghiem, and R. Kwok, "Remote Sensing of Great Lakes Ice Cover Using RADARSAT SAR Data," *CGLAS/CILER Symposium*, University of Michigan, Ann Arbor, MI, February 4, 1997.

[18] G. A. Leshkevich, S. V. Nghiem, and R. Kwok, "Early Results on RADARSAT SAR Applications to Great Lakes Ice," *The Sixth Workshop of the Canadian Ice Working Group, RADARSAT for Ice and Oceans*, Ottawa, Canada, November 19-21, 1996.

B. Meetings

[1] *Remote Sensing for Marine and Coastal Environments*, San Diego, California, October 5-7, 1998: We author and present two papers on Great Lakes experiments, SAR algorithm development, and ice mapping results.

[2] *International Geoscience and Remote Sensing Symposium*, Seattle, Washington, July 6-10, 1998: We author and present two papers on polarimetric radar signatures of various ice types in the Great Lakes and ice identification and classification using SAR data.

[3] *International Association for Great Lakes Research Conference*, Hamilton, Ontario, Canada, May 18-22, 1998: We present a paper on how to interpret satellite SAR data

for Great Lakes ice mapping.

[4] *Remote Sensing and Modeling Great Lakes Ice*, Alexandria, Virginia, October 8-9, 1997: Presented 2 papers on past, present, and future remote sensing of Great Lakes ice. We initiated the potential use of interferometric SAR for three-dimensional mapping of Great Lakes ice including both ice areal coverage and ice thickness. We described the plan to propose to NASA to support airborne interferometric/polarimetric SAR flight (on NASA DC-8 aircraft) experiment over the Great Lakes in conjunction with field experiment with ship and helicopter supported by US Coast Guard and/or Canadian Coast Guard.

[5] *International Geoscience and Remote Sensing Symposium*, Singapore, August 3-8, 1997: Coauthored a paper on *RADARSAT SAR Data Applications*.

[6] *Progress In Electromagnetics Research Symposium*, Cambridge, Massachusetts, July 7-11, 1997: Organized and chaired a special session on *Remote Sensing of the Great Lakes*, in which we presented 2 papers.

[7] *Workshop on Remote Sensing of Planetary Ices: Earth and Other Solid Bodies*, Flagstaff, Arizona, June 11-13, 1997: Presented a paper in the session on *Europa, Sea Ice, and Lake Ice.*

[8] *The Fourth International Conference on Remote Sensing for Marine and Coastal Environments*, Orlando, Florida, March 17-19, 1997: Presented 2 papers in the session on *Air-Sea Interaction and Sea Ice.*

[9] *CGLAS/CILER Symposium*, University of Michigan, Ann Arbor, MI, February 4, 1997: Presented a paper on *Great Lakes Ice Remote Sensing.*

[10] *The Sixth Workshop of the Canadian Ice Working Group*, *RADARSAT for Ice and Oceans*, Ottawa, Canada, November 19-21, 1996: Presented a paper in the session on *Ice.*

IV. PROJECT SUMMARY

A. Milestones

- Initial algorithm and early RADARSAT results (1996)
- Arrangement/coordination for field experiment (1996-1997)
- Modification JPL C-band radar configuration for USCG ship (1997)
- Completed software for shipborne radar control and radar data acquisition (1997)
- Field Experiments - Obtained about 2000 radar data sets and collected ground truth for various ice types (1997)
- Completed shipborne radar data processor with full calibration algorithm (1997)
- Algorithm (supervised selection of training data sets) using field-experiment training ice areas for uncalibrated RADARSAT data (1997)
- Ice map from RADARSAT imagery (1997)
- Shipborne radar data processing and calibration for various ice types (1997-1998)
- Algorithm (automatic) using lookup table from backscatter signature library of various ice types for ERS data (1998)
- Ice map from ERS imagery (1998)

B. Budget

The total budget for FY98 includes $80K for the Jet Propulsion Laboratory and $18K for NOAA Great Lakes Environmental Research Laboratory, the same as in the original proposal (JPL Task Plan No. 80-4237, NOAA Assigned Project No. 56).

C. Period of Performance

The period of performance for FY98 has been extended to November 1998.

V. PROJECT OUTLOOK

A. Outlook

While the present task plan develops the basic algorithm for the Great Lakes ice cover mapping using RADARSAT and ERS SAR data with extensive field experiment data and observations. There are issues that have not been included in the scope of this short-term task plan. These issues can be addressed in a continuing follow-on task plan. Furthermore, the results from this project lead to promising outlook for the remote sensing of the Great Lakes ice cover. We discuss these subjects as follows:

1. *Ice Mapping Issues:*

   The first issue is diurnal effects. RADARSAT ans ERS satellites are on (near) sun synchronous orbits which overpass a given location on the Great Lakes along ascending and descending orbit paths at daytimes and nighttimes. Since the solar radiation and temperature can induce changes in snow covered ice, the backscatter for the same ice type may appear different at different times of the day. The change depends on several factors including the magnitude of the change in environmental parameters at different times and the time delay of thermal response in ice. Thus, the sensitivity of backscatter to diurnal cycles needs to be determined. The results on the diurnal backscatter sensitivity will dictate whether the diurnal effect needs to be incorporated in the ice algorithm. *The second issue is rain effects.* Rain can have a strong impact on backscatter signature of ice. This effect is not just simply the trans-atmospheric radar wave attenuation introduced by rain. Rain increases the wetness of the ice surface or the snow cover. The surface wetness can increase surface scattering while subdues volume scattering from snow ice layers. Consequently, ice backscatter signature changes. The change is different at different polarizations and the copolarized ratio of the backscatter may be reversed. Radar backscatter measurements over snow ice and lake ice with dry snow cover were taken at several locations during the Mackinaw expedition. Only one case of wet snow cover was measured for backscatter signature during the Biscayne Bay experiment. This case can be studied to make an initial assessment of the rain impact on ice backscatter and further measurements and observations are necessary. *The third issue is seasonal changes.* Over a given winter season, the ice growth, environmental conditions, and physical characteristics of ice in the lakes vary from freeze-up in early winter to break-up in late winter. For example, total snow accumulation on lake ice changes throughout the winter season affecting the radar backscatter from lake ice. Higher temperatures and insolation in late winter increase snow wetness and modify the radar return. To account for these effects, data from several winter seasons need to be used to extract statistically meaningful results. *The next issue is the interannual variability.* The total degree-days and snow fall vary from year to year. These factor affects the distribution between snow ice and lake in the total ice thickness distribution. Thus, an interannual bias may need to be introduced in the ice algorithm to obtain consistent results. This study requires long-term calibrated data from the same sensors to avoid artificial biases caused by changes or drift in sensor characteristics. *Another issue is lower latitude ice (in lower lakes).* The 1997 winter were carried out over northern Lake Michigan and over Lake Superior. The results are valuable because the experiments cover the usual navigation routes opened by the USCG ice breakers. However, ice in lake locations at lower latitudes are also important such as the St. Clair River area, which is susceptible to flooding caused by ice jam. Ice mapping needs to be accurate in such particular areas at lower latitudes to provide accurate input ice coverage parameters to flooding forecast models. Thus, the applicability of backscatter signatures for ice mapping between higher and lower latitude ice needs to be examined. This is because ice at different latitudes is subject to different local weather conditions during the winter, which cause differences in the ice growth and ice physical characteristics.

2. Application of Interferometric SAR for Three-Dimensional Ice Mapping over the Great

Lakes:

The 1997 experimental results show that C-band radar can propagate through the typical ice thickness on the Great Lakes. This radar penetration capability is fundamental for radar waves to carry information on ice thickness. NASA has approved our proposal to carry out interferometric airborne SAR experiment on NASA DC-8 aircraft over the Great Lakes during winter (Dr. E. D. Paylor, NASA Headquarters). NASA will fund DC-8 aircraft flights, interferometric and/or polarimetric airborne SAR system operations at multiple frequencies (C-band, L-band, and P-band) and multiple incidence angles (20 to 50 degrees), SAR data acquisition, and interferogram and polarimetric radar image products. The flight schedule is not decided and still needs to be arranged. The U.S. Coast Guard has approved continuing support for the USCG ship and helicopter use (Captain T. S. Sullivan, by direction of Commander, 9th Coast Guard District). The Canadian Coast Guard also indicates that the Canadian ship (the CCGS Samuel Risley) can be used in the experiment (Tom Anderson, Sup. Icebreaking, Canadian Cost Guard). The U.S. National Ice Center has indicated that ice thickness mapping products are important and NIC is supportive of the efforts to demonstrate the ice thickness measurements with interferometric SAR (Commander D. L. Martin, Director, NIC). The Canadian Ice Service has expressed the interest to participate in the field experiment (Ken Armus, CIS). The Great Lakes Research Consortium has identified ice coverage and ice thickness to be among the most important parameters that need to be determined (Professor H. Shen et al., Publication [3] above).

3. *Application of spaceborne NSCAT (NASA Scatterometer) radar data to Great Lakes ice mapping:*

In the results discussed above, we have shown that dual polarization HH and VV data are appropriate for ice mapping regardless of wind speed over open water. We have applied the approach to demonstrate the ice mapping with NSCAT data. NSCAT is a spaceborne radar operated at Ku band. NSCAT coverage is excellent (full-swath covering the entire globe in 2 to 3 days); however, the resolution is much coarser (25 km by 7 km) compared to satellite SAR. As an example, we enclose two NSCAT copolarization ratio images (blue is open water), which compare relatively well with Great Lakes ice charts from NIC in the same time periods. NSCAT operation was terminated by middle 1997. However, NASA follow-on missions have been in preparation including QuickScat to be launched in 1999 and SeaWinds to be launched soon afterward. Even though scatterometer resolutions are coarse, the data can be used to supplement SAR data in terms of coverage and observation frequency (increasing temporal resolution). Ice mapping products from scatterometer data can be used to produce ice cover animation video for the entire winter season and the data set will be useful for climate studies.

4. Application of spaceborne ENVISAT SAR data to Great Lakes ice mapping:
Again, as our C-band radar data indicate the use of copolarization ratio for Great Lakes ice mapping, ENVISAT SAR data which have both HH and VV backscatter with a high resolution are excellent. We have submitted a proposal for the European Space Agency to support the ENVISAT SAR data acquisitions over the Great Lakes and SAR data products to be supplied to us with no charge. We propose to obtain SAR data in dual polarization image modes at large incidence angles, where our measurements show that the differences between HH and VV are larger (with HH larger than VV) for typical Great Lakes ice. Note that polarimetric data to be obtained at C-band by the NASA aircraft SAR (discussed above) will be valuable to evaluate the use of the multiple polarization capability of the satellite ENVISAT SAR for Great Lakes ice mapping regardless of wind speeds and sea states. The ENVISAT SAR also has some interferometric capability with the repeat pass configuration.

B. Collaboration

JPL and NOAA/GLERL have firmly establish a close working collaboration throughout the progress of this project as evident in the productive results in the pass years. We continue to foster such collaboration in the present and future joint research on the Great Lakes ice mapping between these institutions. We also have the great support for the

United Sates Coast Guard from ground station, to shipborne experiments, and to airborne ice reconnaissance. These collaborations are important to the success of the present and future research work on the Great Lakes.

C. Projected Resources

For the outlook year studies, it is of the first importance to obtain a continuous data stream of SAR data from present satellite such as RADARSAT and from future satellites such as ENVISAT and RADARSAT-II for the continuing development, improvement, and application of the ice mapping over the entire Great Lakes. The full NSCAT data set is already available at JPL and is ready to be applied to Great Lakes ice cover mapping. The USCG facilities such as ship, air, and ground stations are necessary for field experiments to validate the ice mapping over the Great Lakes. To this objective, NOAA and USCG supports are essential.

REFERENCES

Ice Glossary, U.S. Department of Commerce, National Oceanic and Atmospheric Administration, National Ocean Survey, Lake Survey Center, Detroit, MI (HO 75-602) p.9, 1971.

Laur, H., P. Bally, P. Meadows, J. Sanchez, B. Schaettler, and E. Lopinto, *Derivation of the Backscattering Coefficient* σ^0 *in ESA ERS PRI Products*, ERS SAR Calibration Doc. No. ES-TN-RS-PM-HL09, Issue 2, Rev. 4, 41 p., May 1997.

Leshkevich, G., W. Pichel, and P. Clemente-Colon, "Great Lakes SAR ice research applications demonstration," Proc. of the Second ERS-1 Symp. - Space at the Service of our Environment, Hamburg, Germany, p.675-679, 11-14 October, 1993. ESA SP-361, Jan. 1994.

Leshkevich, G., W. Pichel, P. Clemente-Colon, R. Carey, and G. Hufford, "Analysis of coastal ice cover using ERS-1 SAR data," Int. J. Remote Sensing, 16(17), p. 3459-

3479, 1995.

Lillesand, T. M. and R. W. Kiefer, *Remote Sensing and Image Interpretation*, John Wiley and Sons, New York, 612 p., 1979.

Nghiem, S. V., C-band polarimetric scatterometer: System, operation, sensitivity and calibration, *ONR Sea Ice Electromagnetics Workshop*, Hanover, New Hampshire, September 14-16, 1993.

Nghiem, S. V., R. Kwok, S. H. Yueh, A. J. Gow, D. K. Perovich, J. A. Kong, and C. C. Hsu, “Evolution in Polarimetric Signatures of Thin Saline Ice under Constant Growth,” *Radio Science*, Vol. 32, No. 1, pp. 127-151, January-February 1997.

LIST OF FIGURES

Figure 11: Map of classified ice types derived from the ERS SAR image in Figure 10 using the backscatter signature library together with the level slicing classification method. Yellow is for consolidated ice floes, red for brash ice, green for patchy snow cover on snow ice covered black ice, and other colors for unidentified types.

Figure 12: ERS SAR image (copyright ESA 1997) taken on 22 March 1997 over north central Lake Superior. The elongated feature in the middle of the image is Isle Royale.

Figure 13: Map of classified ice types derived from the ERS SAR image in Figure 12 using the backscatter signature library together with the level slicing classification method. Yellow is for consolidated ice floes, red for brash ice, green for patchy snow cover on snow ice covered black ice, and other colors for unidentified types.


March 20, 1996
LAKE SUPERIOR
copyright CSA 1996
M000652401.sard

Fig. 1

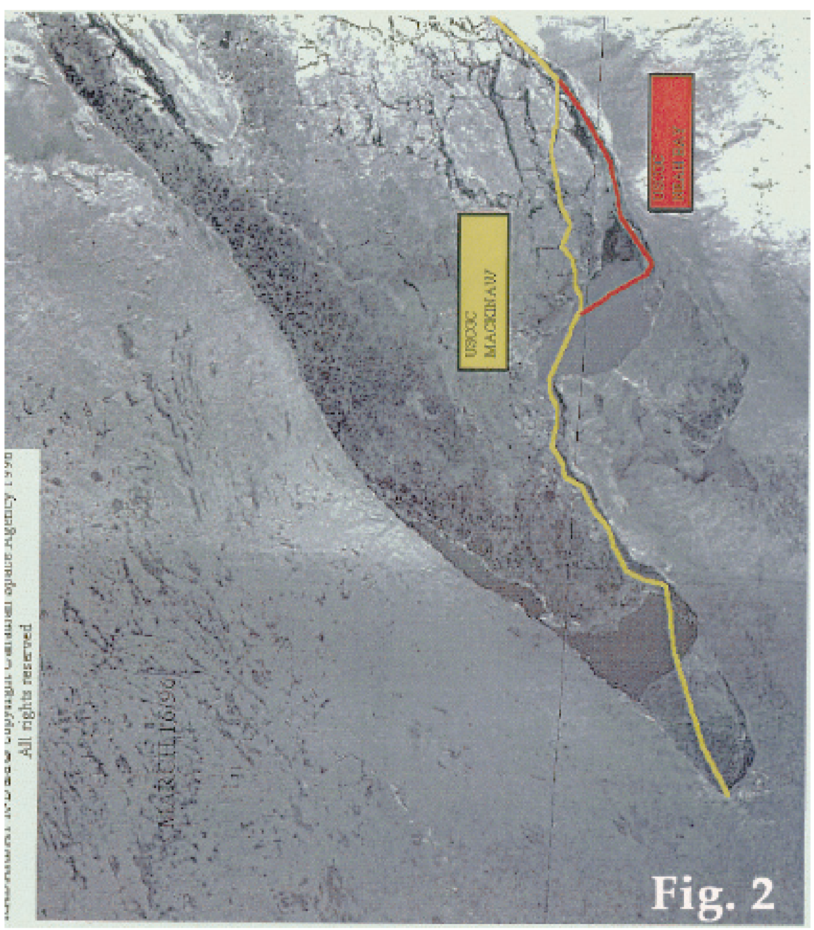
USCGC
MACKINAW
All rights reserved

Fig. 2


20 13:35

Fig. 3

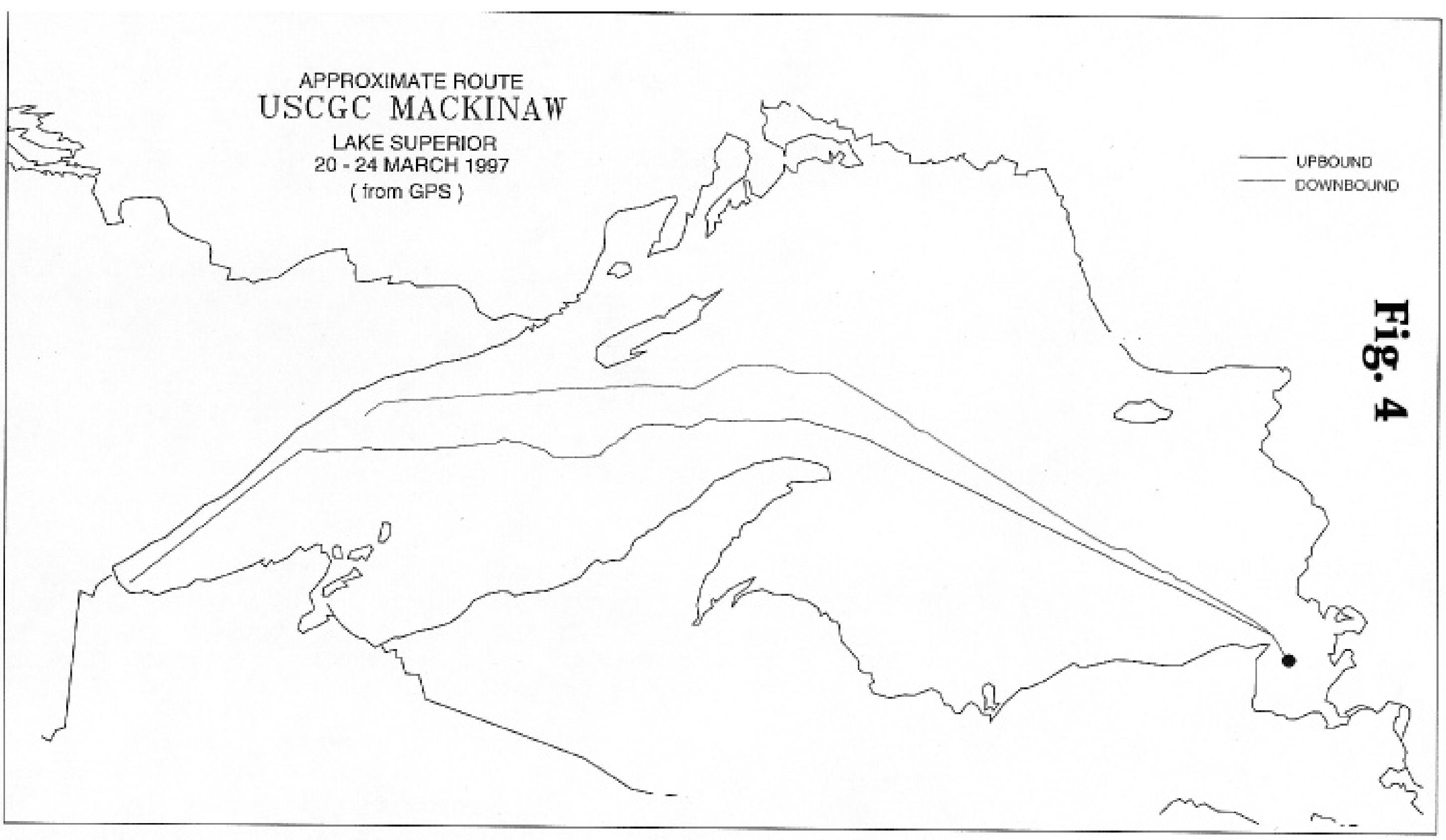
APPROXIMATE ROUTE
USCGC MACKINAW
LAKE SUPERIOR
20 - 24 MARCH 1997
(from GPS)
UPBOUND
DOWNBOUND

Fig. 4

Fig 6.

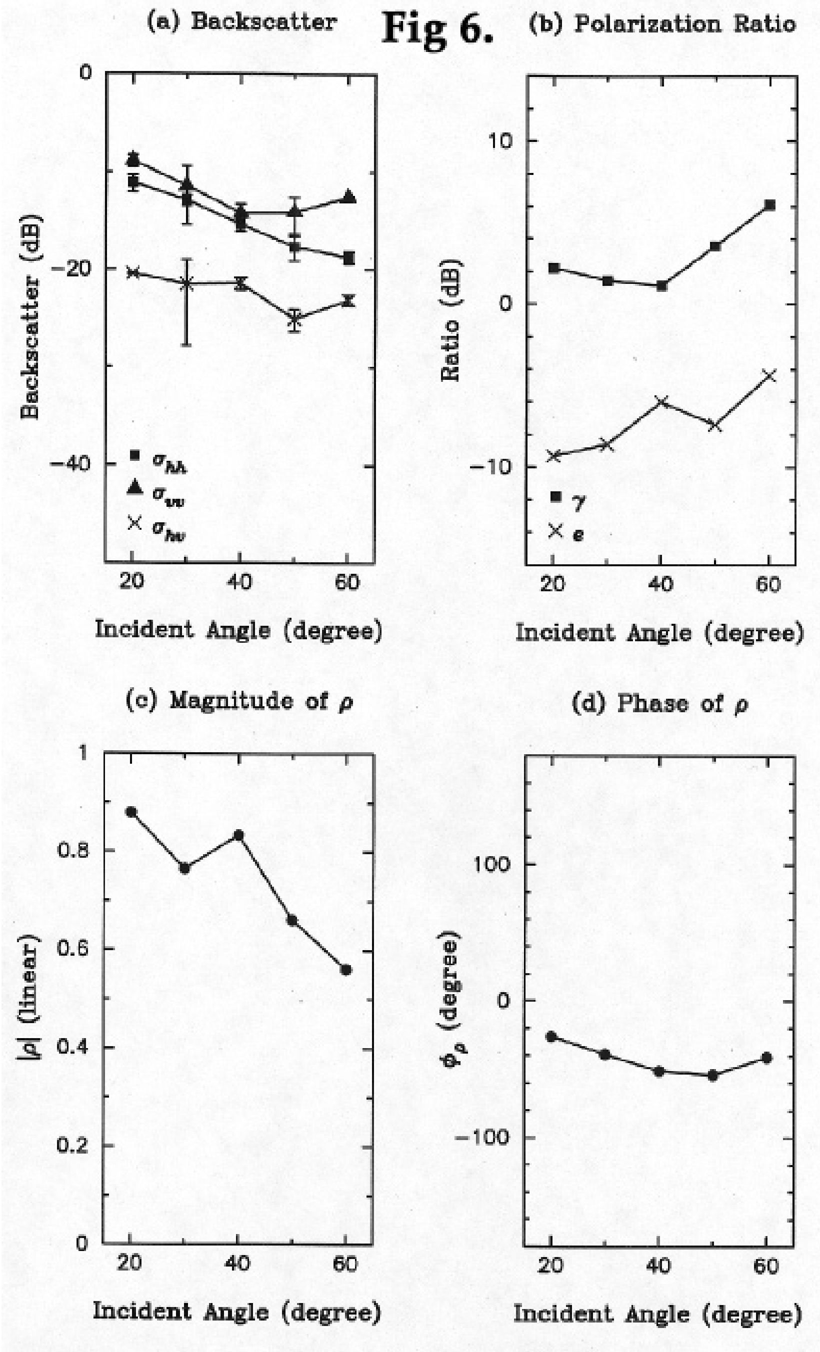
(a) Backscatter
Backscatter (dB)
0
−20
−40
σ_{hh}
σ_{vv}
σ_{hv}
20
40
60
Incident Angle (degree)
(b) Polarization Ratio
Ratio (dB)
10
0
−10
γ
e
20
40
60
Incident Angle (degree)
(c) Magnitude of ρ
$|\rho|$ (linear)
1
0.8
0.6
0.4
0.2
0
20
40
60
Incident Angle (degree)
(d) Phase of ρ
ϕ_ρ (degree)
100
0
−100
20
40
60
Incident Angle (degree)


Fig. 5

Fig. 8

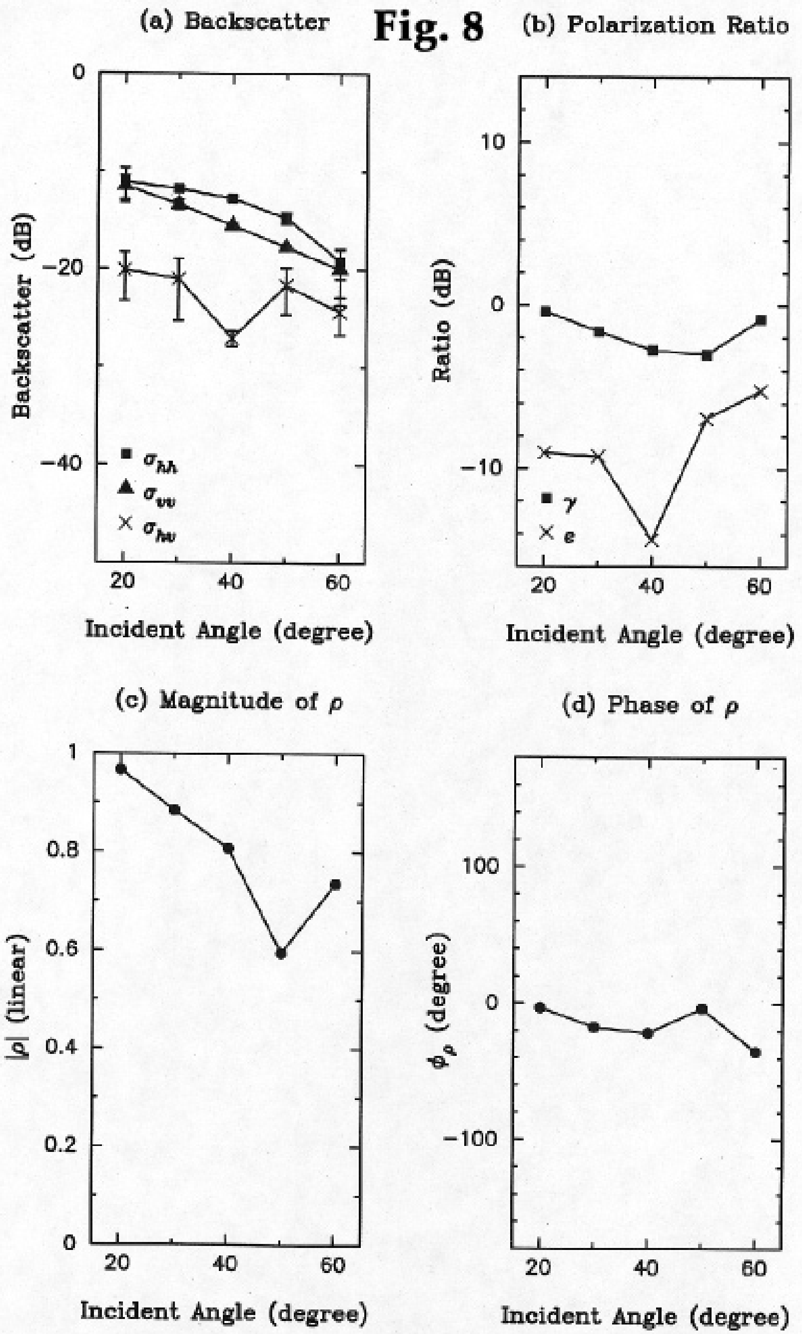

(a) Backscatter
Backscatter (dB)
0
-20
-40
σ_{hh}
σ_{vv}
σ_{hv}
20
40
60
Incident Angle (degree)
(b) Polarization Ratio
Ratio (dB)
10
0
-10
γ
e
20
40
60
Incident Angle (degree)
(c) Magnitude of ρ
$|\rho|$ (linear)
1
0.8
0.6
0.4
0.2
0
20
40
60
Incident Angle (degree)
(d) Phase of ρ
ϕ_ρ (degree)
100
0
-100
20
40
60
Incident Angle (degree)

Fig. 7

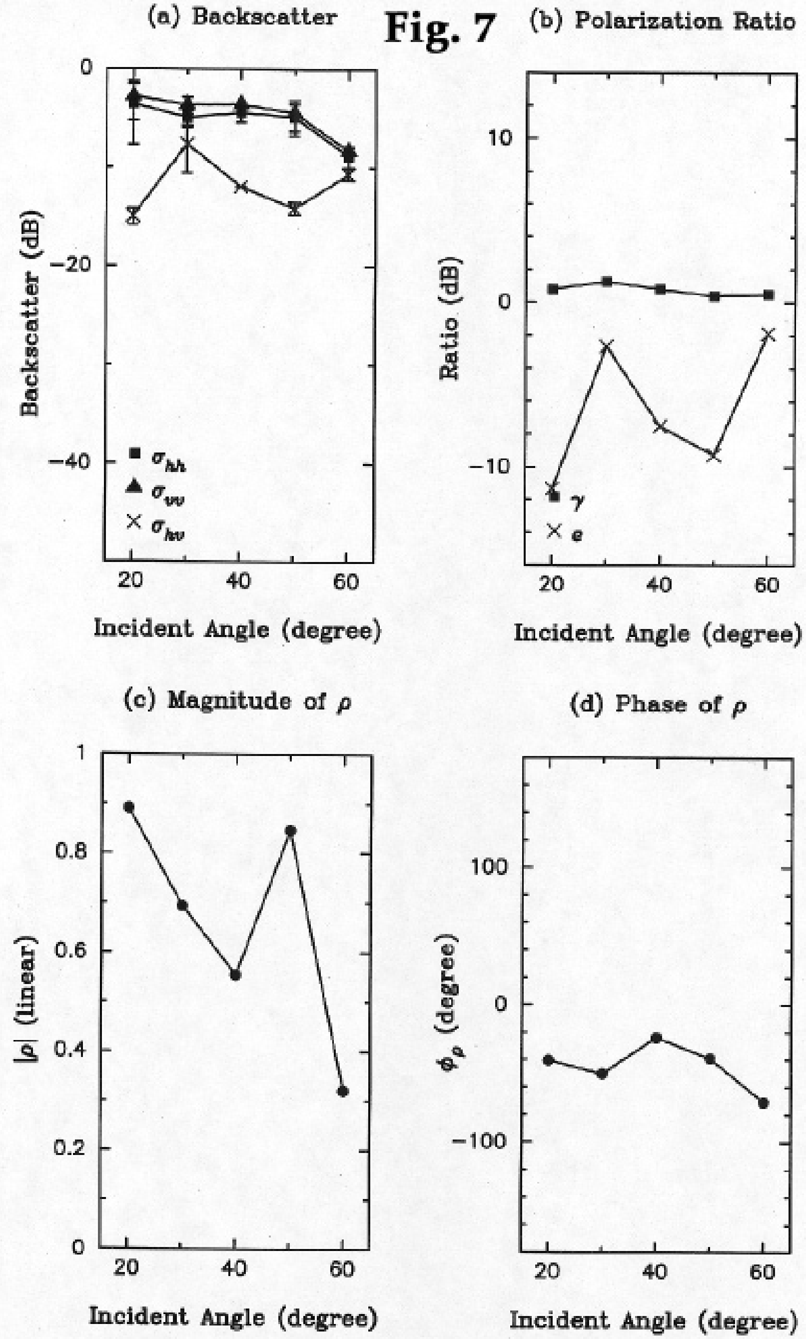

(a) Backscatter
Backscatter (dB)
0
-20
-40
σ_{hh}
σ_{vv}
σ_{hv}
20
40
60
Incident Angle (degree)
(b) Polarization Ratio
Ratio (dB)
10
0
-10
γ
e
20
40
60
Incident Angle (degree)
(c) Magnitude of ρ
$|\rho|$ (linear)
1
0.8
0.6
0.4
0.2
0
20
40
60
Incident Angle (degree)
(d) Phase of ρ
ϕ_ρ (degree)
100
0
-100
20
40
60
Incident Angle (degree)

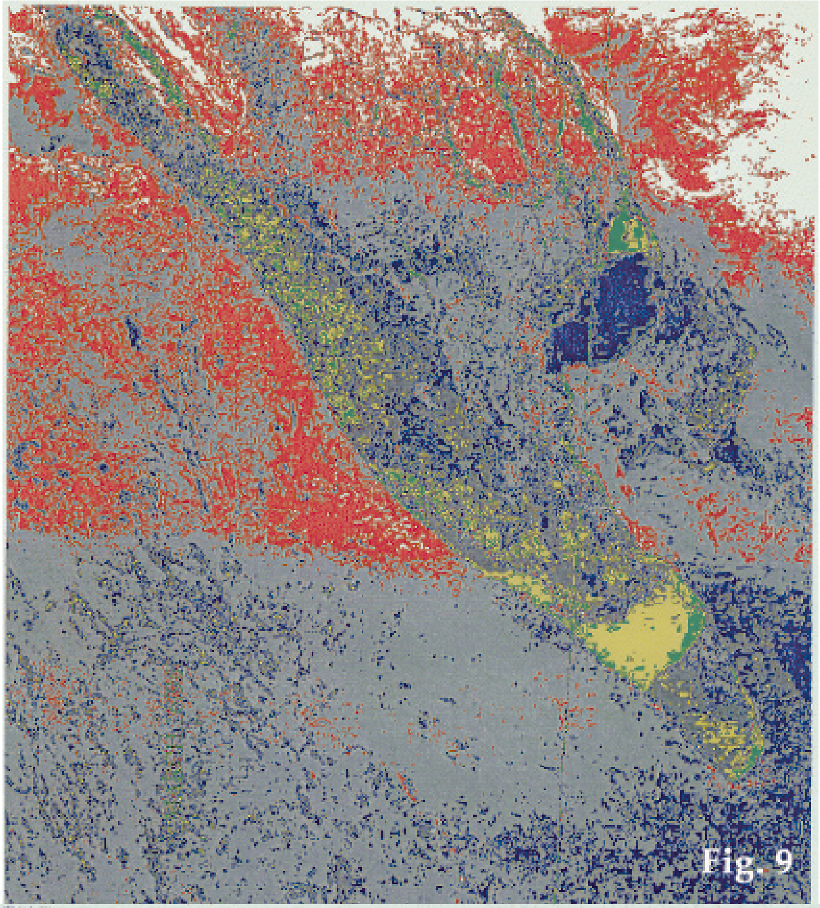
Fig. 9

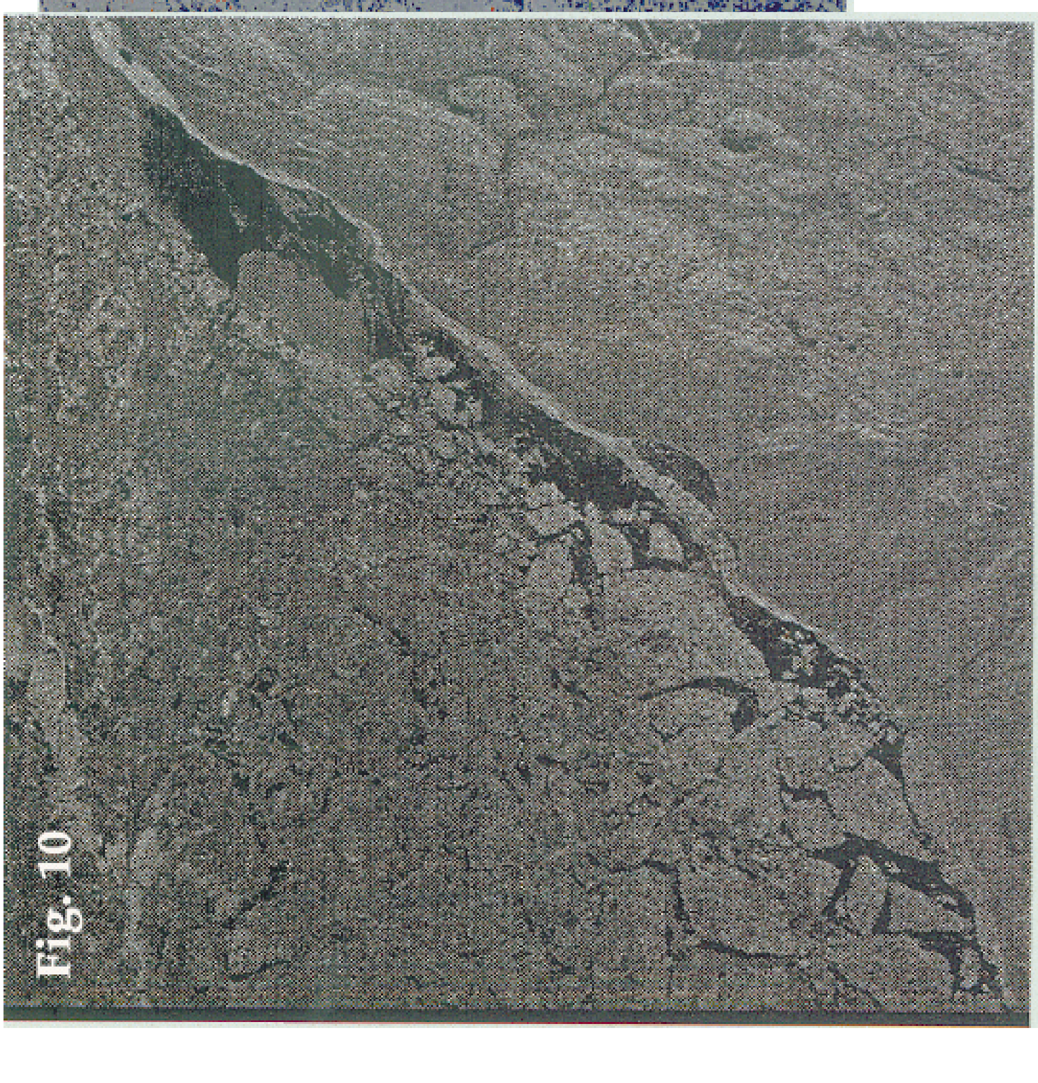
Fig. 10

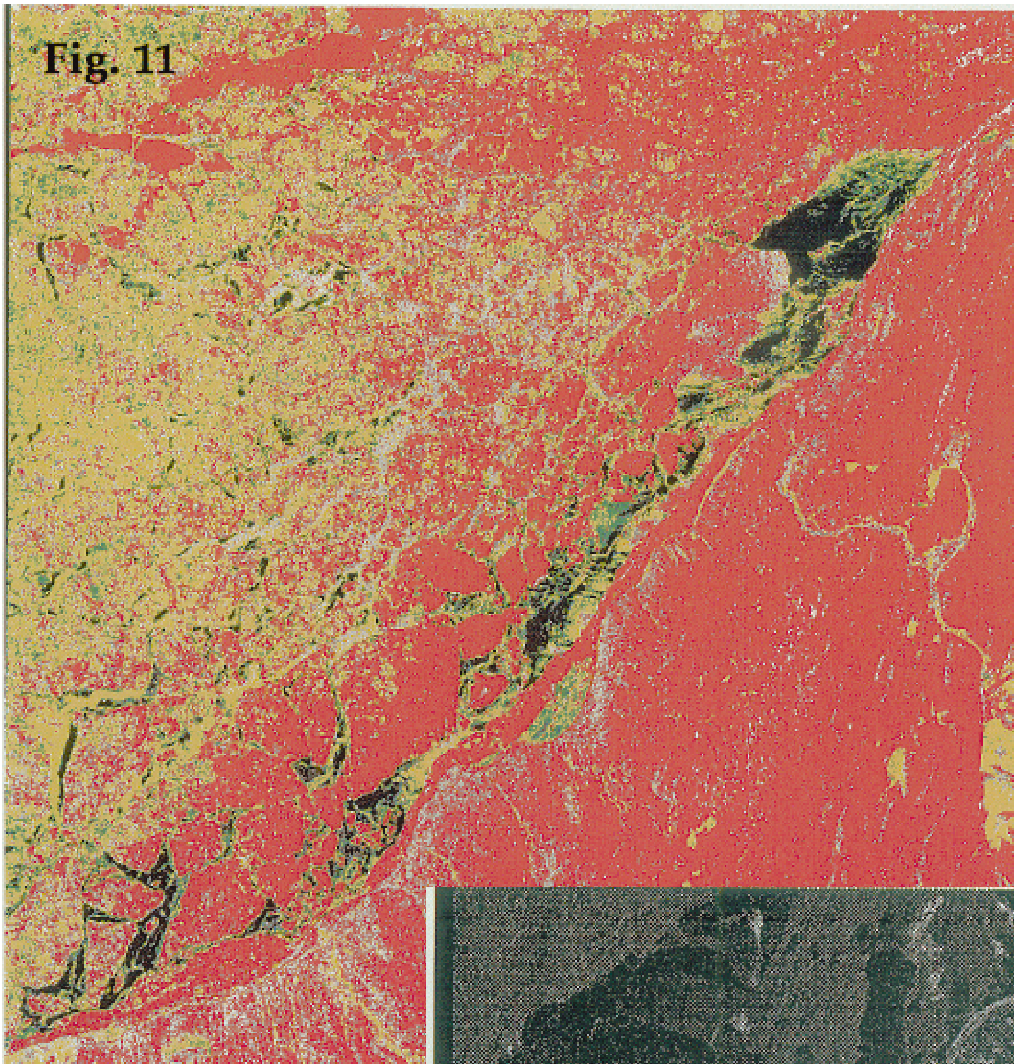

Fig. 11

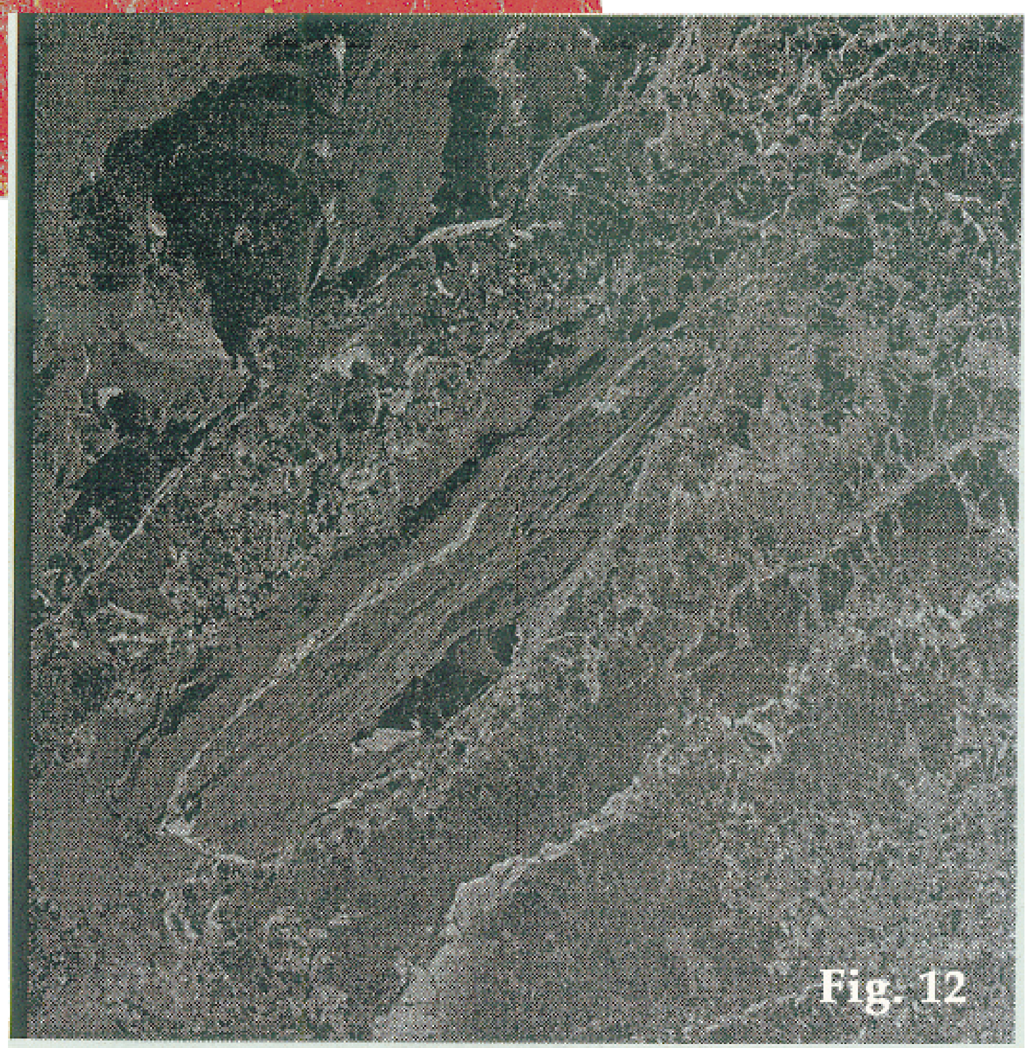

Fig. 12

Fig. 13